Aerodynamic Profile Modification of a NACA 0012 Aerofoil for Enhanced Lift-Drag Characteristics at Low Reynolds Number

Anupam Krishnan[1], Sukanta Roy[2]

[1]Assistant Engineer, Kerala Water Authority, Palakkad, Kerala, India-678001 (anupamkrishnan91@gmail.com) ORCID 0000-0003-2515-8931; [2]Senior Lecturer & Head of Department, Department of Mechanical Engineering, Faculty of Engineering and Science, Curtin University, CDT 250, 98009 Miri, Sarawak, Malaysia (sukanta.roy@curtin.edu.my) ORCID 0000-0002-4762-1352

Abstract

This article discusses the enhanced lift-drag ratio of a geometrically modified National Advisory Committee for Aeronautics 0012 aerofoil at a low Reynolds number of 40000. The study involves validating the Reynolds Averaged Navier Stokes Transition Shear Stress Transport model for the analysis of flow around the subject aerofoil with the modified profile for angles of attack ranging from 0 to 10°. The coefficient of lift to drag increased by 70% for the modified aerofoil at an angle of attack of 6°. The extent of the laminar separation bubble on the modified airfoil is reduced by 40% compared to the standard aerofoil at an angle of attack of 8°. The modified aerofoil cross-section does not involve much manufacturing complexity and can be deployed in small-scale wind turbines operating at low wind speeds.

Author Keywords. NACA 0012, Small-scale Wind Turbine Blade, Transition SST, RANS Simulation, Low Reynolds Number Aerofoil.

Type: Research Article

∂ Open Access ☑ Peer Reviewed ⓒ① CC BY

1. Introduction

Renewable energy projects are gaining more importance with the tremendous increase in the depletion rate of fossil fuels. Fossil fuels are excessively used for transportation and production of electricity which contributes mainly to the amount of greenhouse gases proclaiming the need for a cleaner energy method, such as wind energy. A lot of research is being undertaken in the design of wind turbine blades to increase efficiency. Recent developments in power electrical devices have made wind turbines even more feasible with minimal energy losses. Wind Energy has become one of the most harnessed renewable energy sources due to its availability and good energy density (Anant Kishore and Priya 2013).

The fact that the total capacity of wind energy installations increased by a value of 60.4 Giga Watt (GW, 1 billion watts) in the year 2019 is a testimonial to wind energy being a more than viable green energy option. The installed global wind power capacity has risen to 651 GW, of which 72% is contributed by merely five countries, which is indeed a matter of concern. The stop-go policies of nations need to be revamped to boost the wind energy economy worldwide (Lee and Zhao 2020).

Installation of Large-Scale Wind Turbine (LSWT) to produce as much as 15% of the global energy demand will increase the earth's surface temperature by 1°C within 60 years. The climatic effects increase with increased power production and decreased efficiency. On the other hand, Small Scale Wind Turbine (SSWT) is an attractive option for stand-alone and utility

applications because of its smaller diameter of 3 to 10 m. Blade Element Momentum theory is the traditional method used to predict the performance of a wind turbine, mostly restricted to large-scale ones. With the unfolding of powerful computational facilities, Computational Fluid Dynamics (CFD) became a tool for accurately predicting flow around a wind turbine. Apart from geometry, flow Reynolds number (Re) affects the wind turbine aerodynamics. The power produced from a wind turbine is critically affected by the design of turbine blades. But most investigations are primarily concentrated on LSWTs, which require a lot of space and investment for installation. SSWTs generally work at an area where the wind speed is not optimum, making the aerodynamic design of the turbine blade even more critical (Tummala et al. 2016). Geographical regions where the wind speed is not optimum may require both natural and artificial wind energy sources for power generation. Exhaust air sources such as an air conditioner outlet and ventilation outlets make SSWT highly suitable to an urban environment. The retrofit ability of the same is an added advantage (Gopinath, Suresh, and Kirubakaran 2015).

Depending upon the axis of rotation, wind turbines are classified as Vertical Axis Wind Turbines (VAWT, with axis of rotation in the vertical direction) and Horizontal Axis Wind Turbines (HAWT, with axis of rotation in the horizontal direction). VAWT has the advantage of being placed in any direction to wind, unlike HAWT, which requires ideal placement and an expensive yaw mechanism for optimal performance. HAWTs are mostly self-starting and conventionally used in areas of high wind energy potential. When blade parameters are optimized for a SSWT, it can produce a comparable output power to the large turbine blades that are not optimized (Karthikeyan et al. 2015).

The need for harvesting maximum energy from whatever small wind energy potential, especially in urban areas, has led to the development of Small Scale HAWT. A 40 cm diameter Small Scale HAWT, the Small Wind Energy Portable Turbine (SWEPT), was developed for operation at a rated wind speed of 4 m/s. The symmetric National Advisory Committee for Aeronautics (NACA) 0012 aerofoil is used for the above turbine. As per existing literature, the SWEPT is one of the most efficient SSWT with a power coefficient of 32% (Anant Kishore and Priya 2013).

Compared to LSWT, the SSWT produces a lower power co-efficient, making optimizing aerofoils used for construction even more critical. Aerofoil of an SSWT generally operates at a low Re where efficiency takes a deteriorating effect by the formation of Laminar Separation Bubble (LSB). Once the angle of attack is sufficiently high or the Re is low, the bubble's bursting occurs, causing a significant decrease in the lift coefficient of the aerofoil. This phenomenon may lead to the stalling of aerofoils at sufficiently high angles of attack (Worasinchai, Ingram, and Dominy 2011).

A thin cambered plate has better aerodynamic characteristics than a conventional aerofoil at low Re. An approach to controlling the LSB formation in low Re aerofoil is to facilitate momentum diffusivity between the free stream layer and the separated laminar shear layer to induce transition, thereby reducing the bubble drag. Various researchers show that the performance of conventional aerofoils dramatically deteriorates at this flow regime. Flat plates and cambered plates are more effective at these Re numbers for application in SSWTs. Sharp leading edges accelerate the transition to turbulent flow, as shown by a reversed aerofoil configuration. Cambered aerofoils develop a trailing edge separation also which is inferior to the former. The increase in lift characteristics of a cambered aerofoil is negated by the loss of performance when operating at larger incidence angles due to reversed camber (Winslow et al. 2018).

Several methods are adopted for reducing the length of laminar separation bubbles at the suction surface of the aerofoil. Tabulators are added to the upper edge of the aerofoil to fasten the transition and reattachment process. Modifications of the trailing edge, camber line, and thickness are some of the methods employed to optimize the performance of a low Re aerofoil. The thickness and camber have a substantial effect on the performance of a low Re aerofoil. The thinner blades produce better power coefficients (Karthikeyan et al. 2015).

For improving the lift-drag ratio of an aerofoil, many passive methods are used. A flap at an angle at the trailing edge can produce higher lift, but Gurney Flaps at the trailing edge give a better trade-off between lift and drag coefficients. The use of adjustable flaps that can increase the lift to drag ratio and help maintain stability is increasing (Srinivasa Rao, Mahapatra, and Chaitanya Mangavelli 2018). The effect of Vortex Generators (VG) is analyzed at different positions of the recirculation zone. The placement of the VGs just before the recirculation zone significantly reduces the region of detachment. By plotting the pressure coefficient diagram of an aerofoil, VG's presence flattens the pressure plateau at high angles of attack (da Silva and Malatesta 2020; Li et al. 2019). The effect of introducing dimples and bumps of spherical and pyramidical shapes on the surface of a NACA 0012 aerofoil was studied for subsonic flow at varying angles of attack from 0° to 15°. All surface modifications except the pyramidical protrusions increased the lift-drag ratio, but all changes delayed the flow separation and recirculation (Mehtar and Altaf 2021).

CFD simulation of T106C (a high lift, low-pressure turbine aerofoil) blade is conducted using Reynolds Averaged Navier Stokes (RANS) turbulence model with transition and Large Eddy Simulation (LES) method. The results are validated with experimental data (Marty 2014). 2D CFD analysis of S809 Don Somners aerofoil is conducted to compare different turbulent models available. Out of Spalart-Allmaras, Shear-stress transport (SST) k-ω, and transition SST models, the transition model is more suitable for predicting flow separation at low Re flows and low angle of attacks. But apart from that, the other models were able to predict the flow phenomenon satisfactorily. The LES model predicts the LSB with better accuracy, but the numerical cost associated is almost 1000 times higher, making its use extremely limited. Turbulence needs to be addressed when analyzing such flows, and the three standard methods used are LES, Direct Numerical Simulation (DNS), and RANS. Along with selecting a turbulent model for CFD analysis of an aerofoil, mesh refinement study is also an essential factor. The fineness and properties of the mesh can significantly affect the prediction of lift and drag coefficients of an aerofoil (Sanei and Razaghi 2018).

The aerofoil geometry plays a crucial role in turbine performance and starting characteristics, whether HAWT or VAWT. A good range of maximum lift-drag characteristics is best suited for the VAWT to work effectively at prescribed wind speeds. The aerofoil shows the lowest drag only at narrow-angle of attacks, termed the drag bucket. A wider drag bucket gives better performance when employed in wind turbines. During the early stages of VAWT development, symmetric aerofoils were used, NACA 0012 being one of them. With the commercialization of wind turbines, it became necessary that optimization of an aerofoil be done to improve the efficiency of VAWTs and get comparable efficiencies to that of the HAWTs. During the upwind and downwind rotation, the pressure and suction sides of the VAWT are reversed. Symmetric aerofoils may be deployed to obtain similar performance during both flow directions. Still, as far as starting torque is concerned, cambered aerofoils may be put to good use even though they produce moderate drag when reversal of flow direction occurs. Leading-edge deformation is an effective way for drag reduction in an aerofoil (Anyoji et al. 2014).

In this investigation, a transition-based RANS, the Transition SST model available in commercial CFD package Ansys Fluent, is used for flow analysis at a Re of 40000 for low angles of attack ranging from 0 to 10°. Design modification to the conventional NACA 0012 aerofoil is proposed for an increased lift to drag ratio. The proposed modified aerofoil can be adopted in a low-speed wind turbine blade for improved performance at non-optimum wind conditions. The economic viability of the SSWT depends upon reducing the manufacturing costs of the turbine as well, given the lower efficiency range at which they are working.

2. Computational Method

The behavior of NACA 0012 aerofoil at the selected Re of 40000 is highly non-linear, as already discussed, which calls for turbulence modeling. RANS is one of the most widely used turbulence models for its robustness and economic viability. Turbulent flows are characterized by small and significant fluctuations in velocity components, which cause changes in transported quantities. Complex geometries and flows make direct numerical simulation extremely difficult, so a time averaged method adopted by RANS is used. The one equation Spalart-Allmaras, the two-equation K-ϵ, and the two-equation K-ω are the commonly used turbulence models used in ANSYS. But for this paper's purpose, the Transition Shear-Stress Transport (Transition SST) model is selected for the analysis. The model provides a more accurate resolution of transition while also saving a lot of computation time.

The transition SST model elaborates upon the traditional SST K- ω model that utilizes the K- ω model near the wall and the K- ϵ model in the far field. Additional terms for intermittency and transition onset, in terms of momentum-thickness Reynolds number and empirical relations is used for defining the transition.

The transport equation of the transition SST model is given by the following (NASA 2011):

$$\frac{\partial}{\partial t}(\rho k) + \frac{\partial}{\partial x_j}(\rho k u_j) = \frac{\partial}{\partial x_j}\left([\mu + \sigma_K \mu_t]\frac{\partial k}{\partial x_j}\right) + \widetilde{P_k} - \widetilde{D_k} \tag{1}$$

$$\frac{\partial}{\partial t}(\rho \omega) + \frac{\partial}{\partial x_j}(\rho \omega u_j) = P_\omega - D_\omega + \frac{\partial}{\partial x_j}\left([\mu + \sigma_\omega \mu_t]\frac{\partial \omega}{\partial x_j}\right) + 2(1-F_1)\,(\rho\sigma_{\omega 2}/\omega)\,\frac{\partial k}{\partial x_j}\frac{\partial \omega}{\partial x_j} \tag{2}$$

In the above equations, k is the kinetic energy (m2s-2) and ω the specific dissipation rate (s-1), $\widetilde{P_k}$ is the generation of turbulent kinetic energy due to mean velocity gradients (m4), P_ω is the generation of ω (kgm-3s-2), $\widetilde{D_k}$ and D_ω are dissipation of k and ω due to turbulence. Both the above equations describe the shear flow involved.

$$\frac{\partial}{\partial t}(\rho \gamma) + \frac{\partial}{\partial x_j}(\rho \gamma u_j) = \frac{\partial}{\partial x_j}\left([\mu + \frac{\mu_t}{\sigma_f}]\frac{\partial \gamma}{\partial x_j}\right) + P_\gamma - E_\gamma \tag{3}$$

$$\frac{\partial}{\partial t}(\rho Re\theta_t) + \frac{\partial}{\partial x_j}(\rho Re\theta_t u_j) = \frac{\partial}{\partial x_j}\left(\sigma_{\theta_t}[\mu + \mu_t]\frac{\partial}{\partial x_j}(Re\theta_t)\right) + P_{\theta_t} \tag{4}$$

P_{θ_t} is the source term for the transition momentum thickness Reynolds number transport equation and σ_f and σ_{θ_t} are constants. The addition of Equations (3) and (4) enables the model to take in to account the differences between high and low turbulence at the interface between the wake behind the barrier and free flow.

3. Validation of the Computational Setup

Further, the selected computational model was validated with experimental results available (Ohtake, Nakae, and Motohashi 2007). The geometry of NACA 0012 aerofoil and the C type domain was modeled using ANSYS Design Modeler as shown in Figure 1 and Figure 2, respectively. The chord length of the symmetric aerofoil is fixed at 1 m, and the computational domain spans 12.5 m upstream and downstream of the aerofoil. Structured meshing, as

shown (Figure 3) was adopted for easy convergence. A Mesh refinement study was conducted for five different meshes, and mesh with 125000 elements was finalized considering computational time and acceptable accuracy. The Y+ is an important criterion that determines the accuracy of the mesh being adopted. For an accurate prediction of the viscous sublayer near the wall of the aerofoil, the first layer of the mesh in the far-field direction needs to be placed inside the sub-layer formed. The Y+ value selected for the adopted mesh was 0.9 (Figure 4). The Semi-circular Domain, including the far-field horizontal wall surfaces, is taken as the inlet and the right edge of the domain as the outlet. The aerofoil surface is treated as a wall for computational purposes. The Re selected for simulation is 40000. The properties of the fluid are adjusted to obtain the particular Re under consideration.
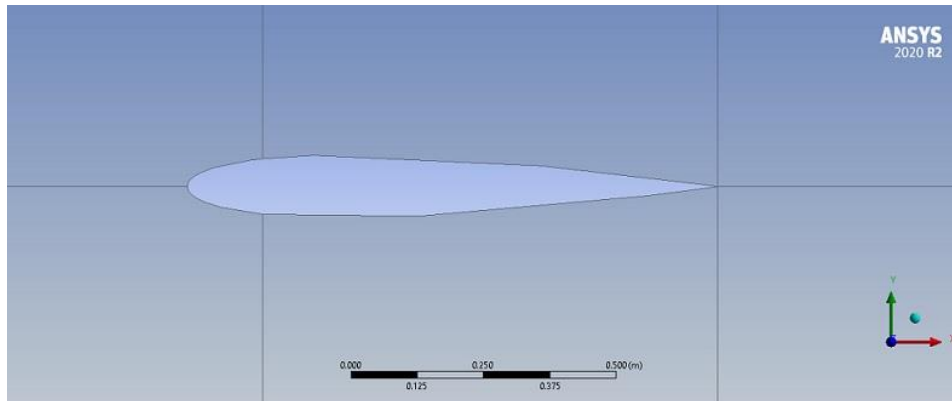

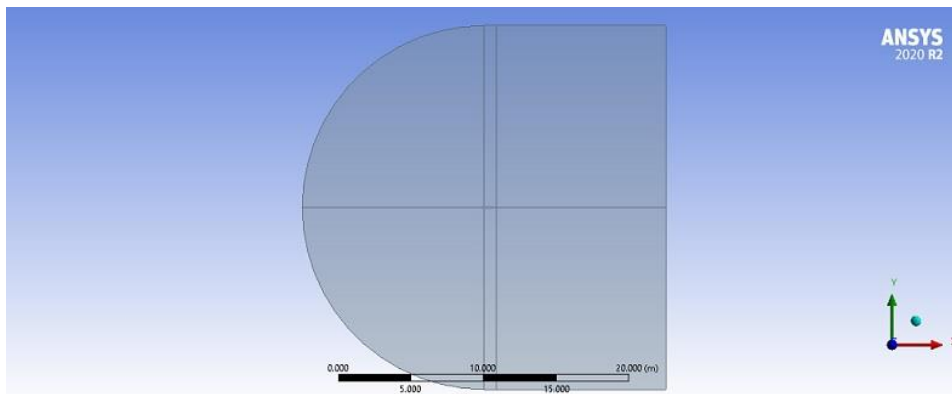**Figure 1**: NACA 0012 aerofoil designed in ANSYS Design Modeler

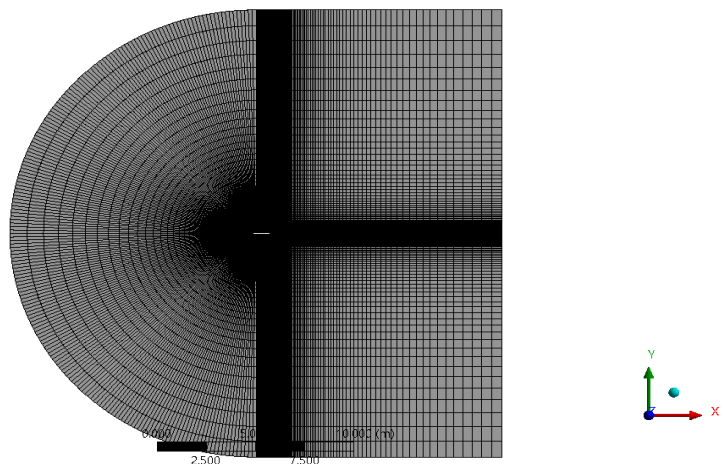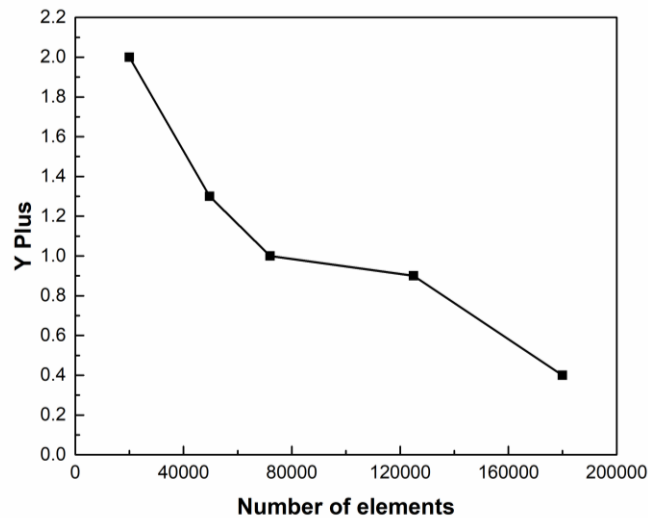**Figure 2**: Fluid Domain over NACA 0012 Aerofoil

Figure 3: Structured Meshing for fluid domain around aerofoil

Figure 4: Variation of Y+ with Number of elements

The model is analyzed for low AOAs from 0 to 10°. RANS simulation for the steady-state problem defined was run for each AOA using the transition SST turbulence model available in Ansys Fluent. The non-dimensional lift and drag coefficients were analyzed for each of the flow criteria. Acceptable results were obtained for the model mentioned above with reasonable computational time involved. The results obtained from simulation were validated using experimental results published (Ohtake, Nakae, and Motohashi 2007). The comparison between lift coefficient and drag coefficient for transition SST simulation setup and experimental values at a Re of 40000 is shown in Figure 5 and Figure 6, respectively. As seen from the plots, it can be seen that the adopted model was giving accurate lift and drag coefficients at tested AOAs, which can provide us an insight into the performance of the NACA 0012 aerofoil at Re = 40000.
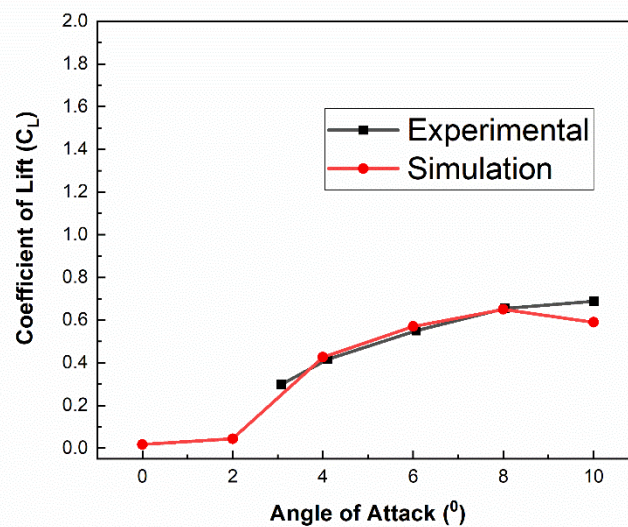
Figure 5: Co-efficient of lift comparison of transition SST simulation with experimental data at Re = 40000 (Ohtake, Nakae, and Motohashi 2007)
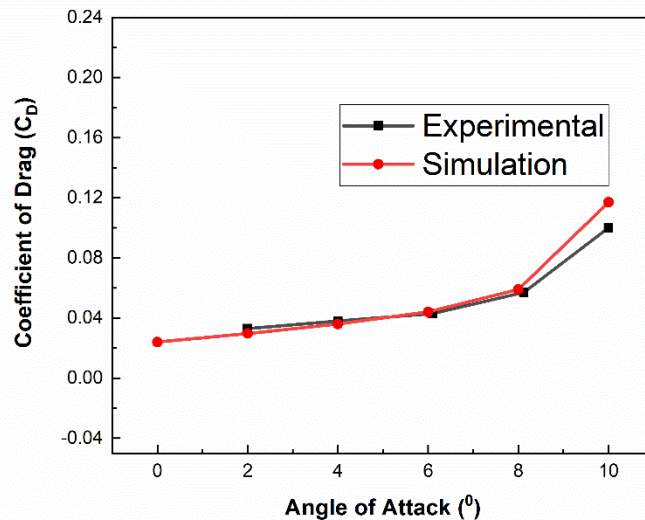
Figure 6: Co-efficient of drag comparison of transition SST simulation with experimental data at Re = 40000 (Ohtake, Nakae, and Motohashi 2007)

4. Design Modification of the Conventional NACA 0012 Aerofoil

The study's objective was to develop a more efficient aerofoil with higher lift-drag ratio for the flow regime, which is essentially laminar and is characterized by flow separation. The proposed aerofoil is a longitudinally cut section of a symmetric NACA 0012 aerofoil, as shown in Figure 7. The flow around the modified aerofoil was analyzed using the already validated computational domain, meshing strategy, and turbulence model for AOAs from 0 to 10°. The mesh generated is shown in Figure 8.
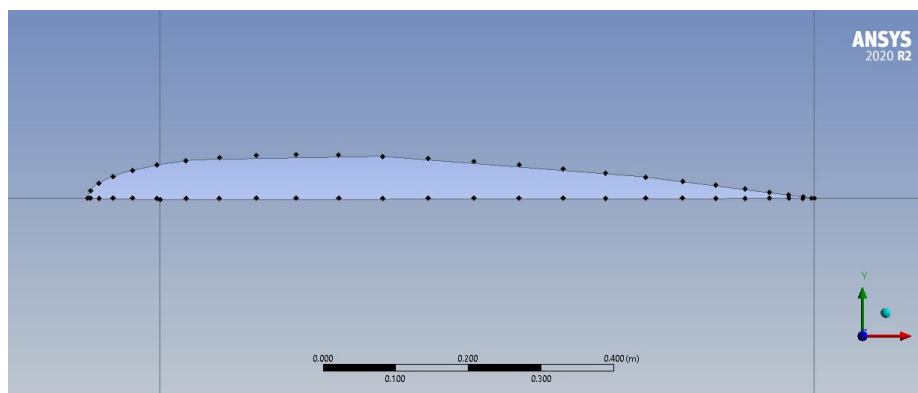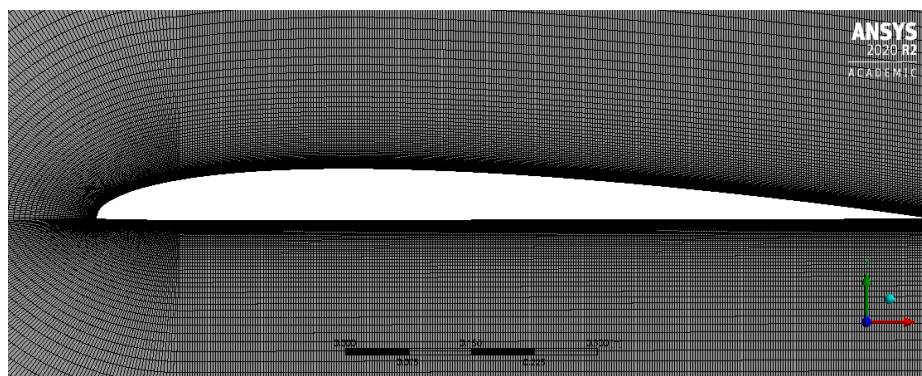

Figure 7: Modified aerofoil cross-section

Figure 8: Structured Meshing for fluid domain around modified aerofoil

5. Results and Discussion

The lift and drag coefficients for the modified aerofoil were compared to that of the NACA 0012 symmetric aerofoil. The modified aerofoil was analyzed for AOA varying from 0 to 10°. As can be seen from Figure 9 and Figure 10, the lift coefficient has improved, and the drag coefficient has reduced for the flow angles considered compared to the conventional aerofoil. The lift to drag ratio of the aerofoils under consideration is plotted in Figure 11. This is obvious from the surface co-efficient of pressure plotted for the angles of attack 6° and 8° as shown in Figure 12. The large suction peak is the source of the high lift generated by the modified aerofoil. This change can be explained by the fact that the modification has made the aerofoil asymmetric, making the suction side more cambered. Flattening of the pressure distribution (plateau) over the suction surface of both the aerofoils verifies that a separation bubble is formed. The skin friction coefficient of both the aerofoil along the suction surface at angles of attack 6° and 8° are plotted in Figure 13. It is seen from the skin friction coefficient data that the extent of the separation bubble zone at the leading edge of the aerofoil is 0.5% of the chord length in the case of NACA 0012 aerofoil. In contrast, it extends to only 0.3% for the modified aerofoil at a larger Angle of Attack of 8°.
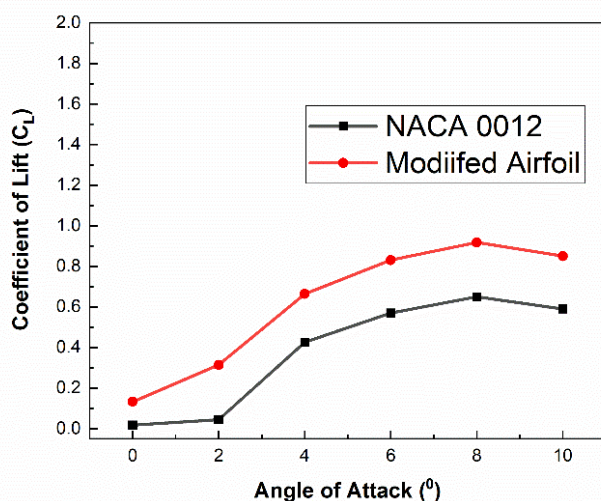

Figure 9: Comparison of co-efficient of lift for NACA 0012 aerofoil with modified aerofoil at Re =40000
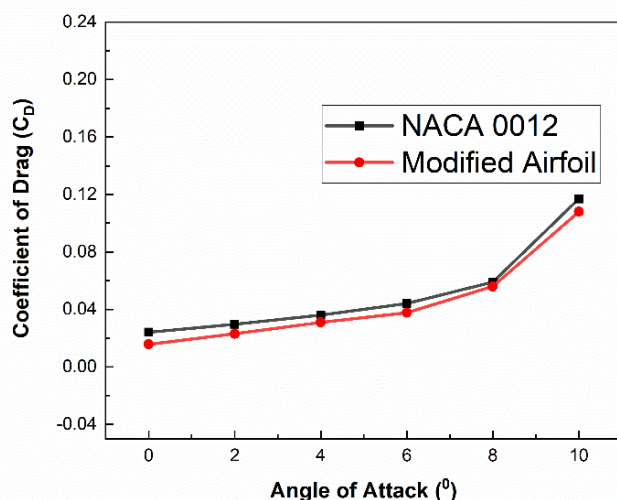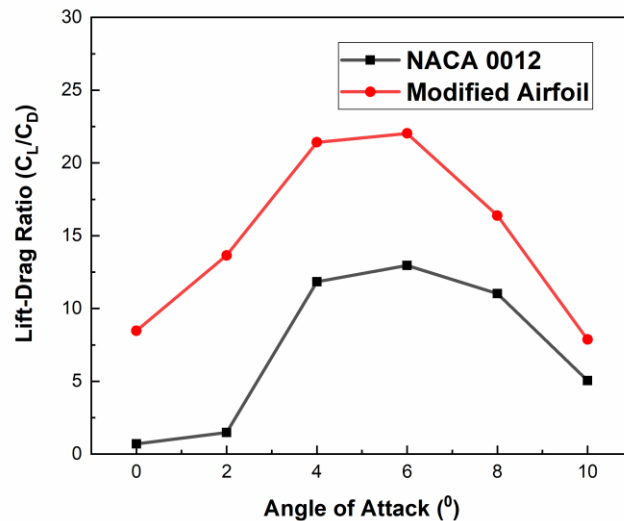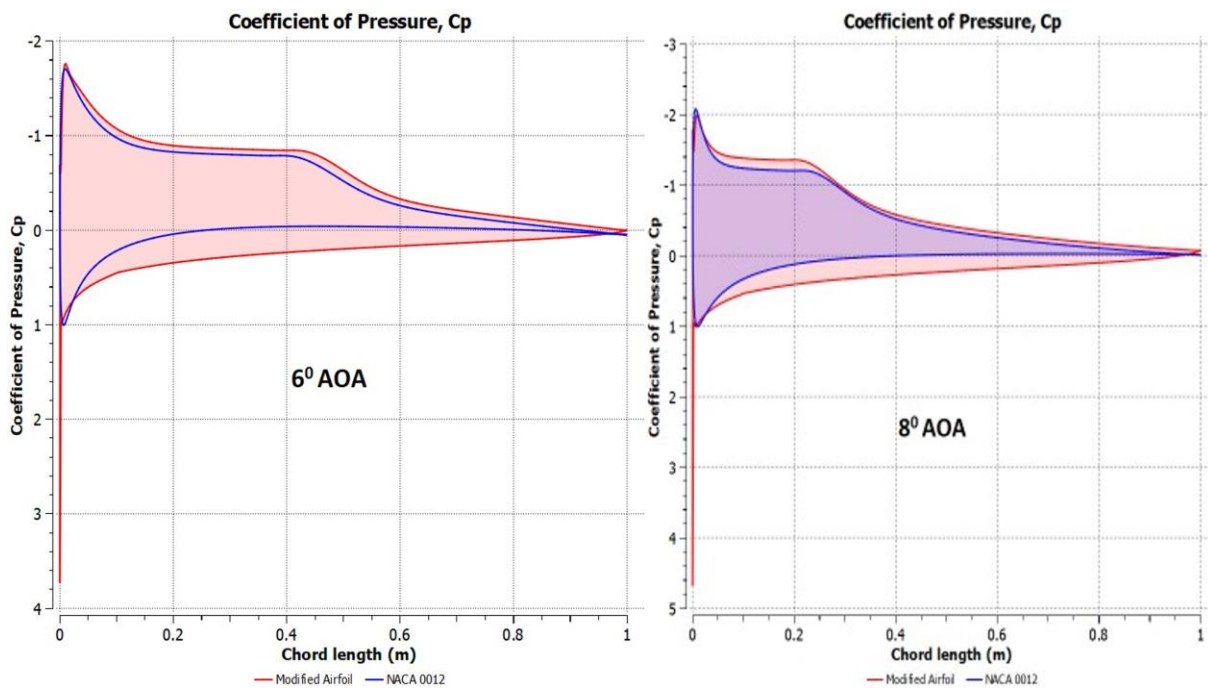

Figure 10: Comparison of co-efficient of drag for NACA 0012 aerofoil with modified aerofoil at Re =40000

Figure 11: Comparison of lift-drag ratio for NACA 0012 aerofoil to modified aerofoil
at Re =40000

Figure 12: Coefficient of Pressure comparison of NACA 0012 & Modified Aerofoils

Even though the effect is not as prominent at the trailing edge, the aerofoil is better off with the modification proposed as far as separation is concerned. The velocity vectors for both the aerofoils at 8° angle of attack are plotted (Figure 14). It can be inferred from the plot that the separation and reattachment zones of the modified aerofoil are shifted towards the leading edge. Also, the extent of the separation bubble is reduced due to the proposed modification. The lift-drag characteristics are superior to the conventional aerofoil, as evident from Table 1 for the flow condition under consideration.
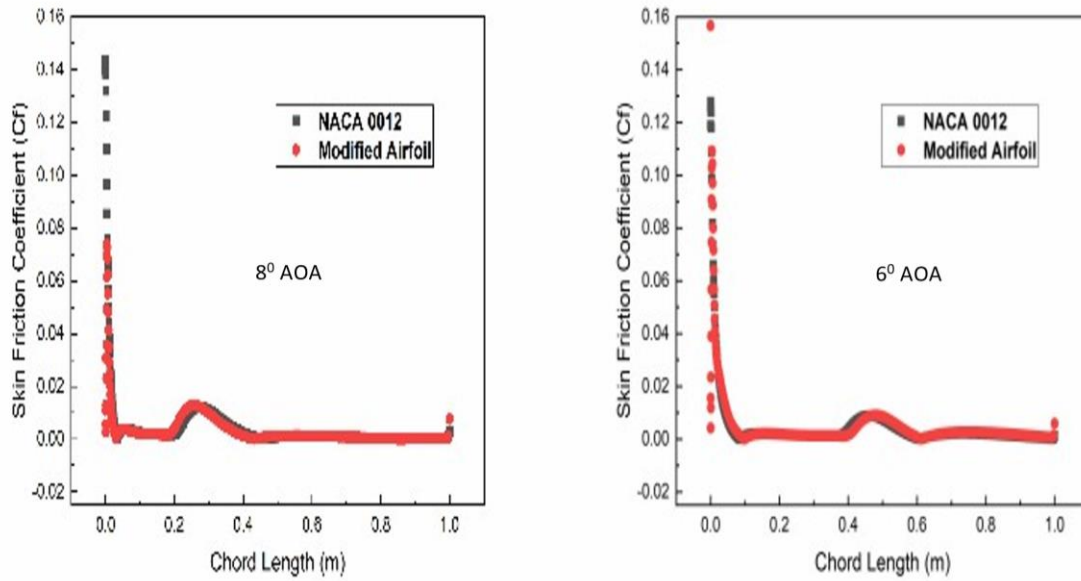
Figure 13: Skin Friction Coefficients across the suction surface of the aerofoils
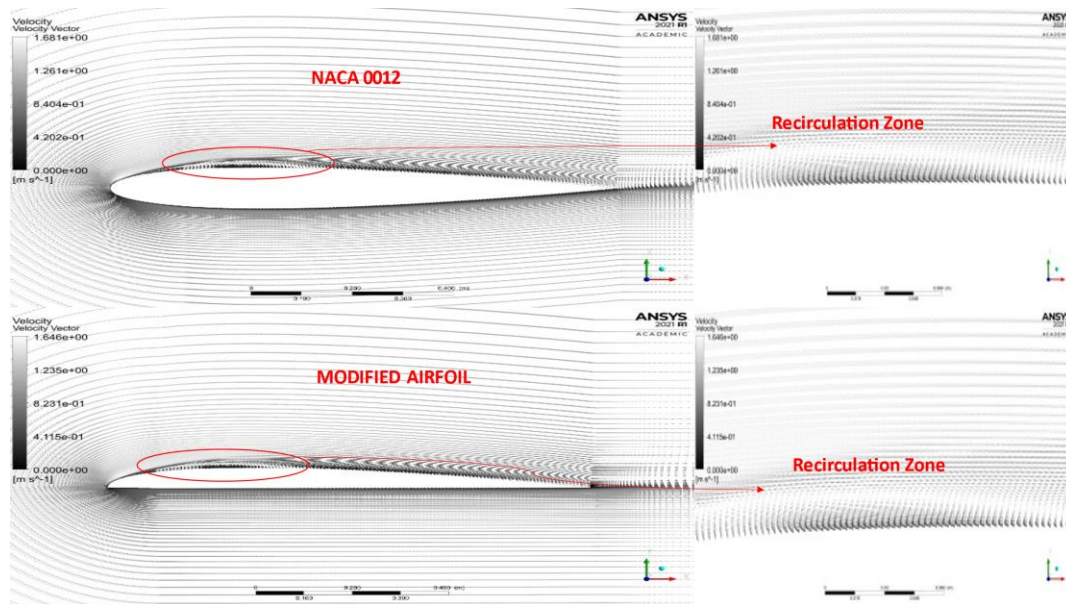

Figure 14: Velocity Vectors for the aerofoils at 8° Angle of Attack

Sl. No.	AOA (°)	NACA 0012			MODIFIED AEROFOIL		
		Co-efficient of Lift	Co-efficient of Drag	Lift to Drag ratio	Co-efficient of Lift	Co-efficient of Drag	Lift to Drag ratio
1	0	0.017	0.024	0.708	0.133	0.0157	8.471
2	2	0.044	0.0297	1.481	0.314	0.023	13.652
3	4	0.426	0.036	11.833	0.664	0.031	21.419
4	6	0.57	0.044	12.955	0.8304	0.0377	22.027
5	8	0.6499	0.059	11.015	0.9175	0.056	16.384
6	10	0.59	0.117	5.043	0.8503	0.108	7.873

Table 1: Comparison of aerodynamic characteristics of NACA 0012 and modified aerofoils

The increase in the camber of the aerofoil while increasing the lift also increases the form drag associated with it. The design modification proposed would be better off than increasing the

aerofoil camber of conventional aerofoils usually used in wind turbine applications. It can be seen that the separation point is further pushed towards the leading edge of the modified aerofoil, thereby allowing the aerofoil to generate more lift and less drag for the Re being considered. The separation point was found to move towards the leading edge with increase in AOA. It is worth noting that the modification proposed does not consume any excess material or energy when compared to other active and passive methods being used to improve the lift to drag characteristics of the conventional aerofoil. The economic viability becomes the prime criterion for the selection of aerofoil for low-speed wind applications as the flow regime already suffers from lower efficiencies when compared to high speeds.

6. Conclusion

The study dealt with improving the lift-drag characteristics of conventional National Advisory Committee for Aeronautics 0012 aerofoil at low speeds. Transition Shear Stress Transport turbulence model was used to analyze flow around aerofoil at a Reynolds number of 40000. The flow analyzed for angles of attack ranging from 0 to 10° was agreeable with already published experimental results. Small Scale Wind Turbine usually works at a low Reynolds number regime which makes the flow more complicated when compared to high Reynolds number flows.

1. A modified aerofoil with a longitudinally cut National Advisory Committee for Aeronautics 0012 cross-section provides a better lift to drag ratio when compared to the initial symmetric aerofoil. The camber and introduction of a sharp leading edge increased the lift for a Reynolds number of 40000.
2. The lift to drag (coefficient) ratio increased by 70% at an angle of attack of 6°. Similar improvements are seen in all the other angles of attack analyzed.
3. The relative pressure difference at the suction and pressure surfaces was increased for the modified aerofoil cross-section. The pressure coefficient plateau is visible in both the aerofoils, confirming the presence of a laminar separation bubble at the Reynolds Number of flow considered.
4. The flow separation effect was found to be relatively less dominant in the modified aerofoil configuration. The point of flow separation was pushed further towards the leading edge of the modified aerofoil.
5. The extent of separation bubble was 0.3% (of the chord length) for modified aerofoil instead of 0.5% for conventional aerofoil at an angle of attack, 8°.
6. The flow separation point was found to be moving towards the leading edge with increase in the angle of attack.

Most of the studies on improving the efficiency of wind turbines have been limited to Large Scale Wind Turbines. The aerofoil profile is also open to optimization, along with geometrical parameters like chord length, twist, and pitch angle. Modifying an aerofoil cross-section can vastly improve Small-Scale Wind Turbines' power coefficient by making them comparable to Large-Scale Wind Turbines. By adopting the modified aerofoil cross-section, the material used for construction can be saved to quite an extent, even though the structural implications are open to investigation. For Small Scale Wind Turbines under consideration, optimization of the aerofoil and the ease in manufacturing is critical for the economic viability of the turbine.

References

Anant Kishore, R., and S. Priya. 2013. "Design and experimental verification of a high efficiency small wind energy portable turbine (SWEPT)". *Journal of Wind Engineering and Industrial Aerodynamics* 118: 12-19. https://doi.org/10.1016/j.jweia.2013.04.009.

Anyoji, M., T. Nonomura, H. Aono, A. Oyama, K. Fujii, H. Nagai, and K. Asai. 2014. "Computational and experimental analysis of a high-performance airfoil under low-Reynolds-number flow condition". *Journal of Aircraft* 51, no. 6: 1864-72. https://doi.org/10.2514/1.C032553.

Gopinath, M. S., V. Suresh, and V. Kirubakaran. 2015. "Performance analysis of turbulent flow horizontal axis micro wind turbine". *International Journal of Energy Technology and Policy* 11, no. 4: 348-57. https://doi.org/10.1504/ijetp.2015.074157.

Karthikeyan, N., K. Kalidasa Murugavel, S. Arun Kumar, and S. Rajakumar. 2015. "Review of aerodynamic developments on small horizontal axis wind turbine blade". *Renewable and Sustainable Energy Reviews* 42: 801-22. https://doi.org/10.1016/j.rser.2014.10.086.

Lee, J., and F. Zhao. 2020. *GWEC Global Wind Report*. Wind Energy Technology. https://gwec.net/global-offshore-wind-report-2020/.

Li, X. K., W. Liu, T. J. Zhang, P. M. Wang, and X. D. Wang. 2019. "Analysis of the effect of vortex generator spacing on boundary layer flow separation control". *Applied Sciences* 9, no. 24. https://doi.org/10.3390/app9245495.

Marty, J. 2014. "Numerical investigations of separation-induced transition on high-lift low-pressure turbine using RANS and LES methods". *Proceedings of the Institution of Mechanical Engineers, Part A: Journal of Power and Energy* 228, no. 8: 924-52. https://doi.org/10.1177/0957650914548741.

Mehtar, Z., and A. Altaf. 2021. "Influence of spherical and pyramidical dimples and bumps on airfoil performance in subsonic flow". *Journal of Aerospace Technology and Management* 13: Article number e3121. https://doi.org/10.1590/jatm.v13.1219.

NASA. 2011. "The Langtry-Menter 4-Equation Transitional SST Model". Langley Research Center. Turbulence Modeling Resource. Updated March 22, 2022. https://turbmodels.larc.nasa.gov/langtrymenter_4eqn.html.

Ohtake, T., Y. Nakae, and T. Motohashi. 2007. "Nonlinearity of the aerodynamic characteristics of NACA0012 aerofoil at low Reynolds numbers". *Journal of the Japan Society for Aeronautical and Space Sciences* 55, no. 644: 439-45. https://doi.org/10.2322/jjsass.55.439.

Sanei, M., and R. Razaghi. 2018. "Numerical investigation of three turbulence simulation models for S809 wind turbine airfoil". *Proceedings of the Institution of Mechanical Engineers, Part A: Journal of Power and Energy* 232, no. 8: 1037-48. https://doi.org/10.1177/0957650918767301.

da Silva, D., and V. Malatesta. 2020. "Numerical simulation of the boundary layer control on the NACA 0015 airfoil through vortex generators". *Journal of Aerospace Technology and Management* 12, no. 1: Article number e1920. https://doi.org/10.5028/jatm.v12.1102.

Srinivasa Rao, T., T. Mahapatra, and S. Chaitanya Mangavelli. 2018. "Enhancement of Lift-Drag characteristics of NACA 0012". *Materials Today: Proceedings* 5: 5328-37. https://doi.org/10.1016/j.matpr.2017.12.117.

Tummala, A., R. K. Velamati, D. K. Sinha, V. Indraja, and V. H. Krishna. 2016. "A review on small scale wind turbines". *Renewable and Sustainable Energy Reviews* 56: 1351-71. https://doi.org/10.1016/j.rser.2015.12.027.

Winslow, J., H. Otsuka, B. Govindarajan, and I. Chopra. 2018. "Basic understanding of airfoil characteristics at low Reynolds numbers (104–105)". *Journal of Aircraft* 55, no. 3: 1050-61. https://doi.org/10.2514/1.C034415.

Worasinchai, S., G. Ingram, and R. Dominy. 2011. "A low-Reynolds-number, high-angle-of-attack investigation of wind turbine aerofoils". *Proceedings of the Institution of Mechanical Engineers, Part A: Journal of Power and Energy* 225, no. 6: 748-63. https://doi.org/10.1177/0957650911405411.